Blocking Triggering Receptor Expressed on Myeloid Cells-1-Positive Tumor-Associated Macrophages Induced by Hypoxia Reverses Immunosuppression and Anti-Programmed Cell Death Ligand 1 Resistance in Liver Cancer

Qinchuan Wu,[1-4]* Wuhua Zhou,[1-4,6]* Shengyong Yin,[2-4]* Yuan Zhou,[1-4] Tianchi Chen,[1-4] Junjie Qian,[1-4] Rong Su,[2-4] Liangjie Hong,[2-4] Haohao Lu,[2-4] Feng Zhang,[2-4] Haiyang Xie,[2-5] Lin Zhou,[1-5] and Shusen Zheng [iD] [1-5]

Tumor-associated macrophages (TAMs) are recognized as antitumor suppressors, but how TAMs behave in the hypoxic environment of hepatocellular carcinoma (HCC) remains unclear. Here, we demonstrated that hypoxia inducible factor 1α induced increased expression of triggering receptor expressed on myeloid cells-1 (TREM-1) in TAMs, resulting in immunosuppression. Specifically, TREM-1-positive (TREM-1+) TAMs abundant at advanced stages of HCC progression indirectly impaired the cytotoxic functions of CD8+ T cells and induced CD8+ T-cells apoptosis. Biological and functional assays showed that TREM-1+ TAMs had higher expression of programmed cell death ligand 1 (PD-L1) under hypoxic environment. However, TREM-1+ TAMs could abrogate spontaneous and PD-L1-blockade-mediated antitumor effects *in vivo*, suggesting that TREM-1+ TAM-induced immunosuppression was dependent on a pathway separate from PD-L1/programmed cell death 1 axis. Moreover, TREM-1+ TAM-associated regulatory T cells (Tregs) were crucial for HCC resistance to anti-PD-L1 therapy. Mechanistically, TREM-1+ TAMs elevated chemokine (C-C motif) ligand 20 expression through the extracellular signal-regulated kinase/NF-κβ pathway in response to hypoxia and tumor metabolites leading to CCR6+Foxp3+ Treg accumulation. Blocking the TREM-1 pathway could significantly inhibit tumor progression, reduce CCR6+Foxp3+ Treg recruitment, and improve the therapeutic efficacy of PD-L1 blockade. Thus, these data demonstrated that CCR6+Foxp3+ Treg recruitment was crucial for TREM-1+ TAM-mediated anti-PD-L1 resistance and immunosuppression in hypoxic tumor environment. *Conclusion*: This study highlighted that the hypoxic environment initiated the onset of tumor immunosuppression through TREM-1+ TAMs attracting CCR6+Foxp3+ Tregs, and TREM-1+ TAMs endowed HCC with anti-PD-L1 therapy resistance. (HEPATOLOGY 2019;70:198-214).

Hypoxia closely associates with malignant progression and poor outcome in almost all solid tumors, especially in hepatocellular carcinoma (HCC).[1,2] Accumulating evidence has revealed that hypoxia accelerates tumor cell proliferation and matrix remodeling through hypoxia

inducible factor 1α (HIF-1α), which regulates the transcription of a variety of oncogenes on oxygen deficiency.[3,4] Therefore, in addition to tumor cells, tumor-infiltrating leukocytes (TILs), and tumor-associated macrophages (TAMs), for instance, are susceptible to oxygen shortage and tumor metabolites, eventually resulting in immunosuppression and tumor escape.[5,6] TAMs are widely present in the tumor microenvironment and are able to promote angiogenesis, cell invasion, and TILs accumulation.[7-9] However, in hypoxic context, the functions of TAMs and their relevant mechanisms of immunosuppression are far less understood.

Studies have shown that up-regulation of triggering receptor expressed on myeloid cells-1 (TREM-1) is observed frequently in dendritic cells and occasionally in TAMs,[10] and TREM-1 has roles in the release of proinflammatory cytokines, and T-cell differentiation, proliferation, and effector responses through the mitogen-activated protein kinase (MAPK)/extracellular signal-regulated kinase (ERK) and NF-κβ pathways.[11] Moreover, TREM-1 has been unveiled as a hypoxia-associated protein involved in dendritic cell (DC) activation.[12-14] However, it is still unclear whether and how HIF-1α regulates TREM-1

expression under hypoxia. TREM-1 has been determined to be an oncoprotein, and TREM-1+ TAMs not only contribute to intestinal tumorigenesis but also correlate with reduced disease-free survival and overall survival in lung cancer.[15,16] Although Kupffer cells with TREM-1 up-regulation have been shown to promote liver carcinogenesis by triggering the release of tumor-associated cytokines,[17] little is known about the potential mechanism through which TREM-1+ TAMs regulate relevant tumor-promoting cytokines. Additionally, a high level of programmed cell death ligand 1 (PD-L1), a canonical immune checkpoint molecule, is correlated with immunosuppression and is frequently affected by various factors. Whether PD-L1 expression is modulated by TREM-1 and the efficacy of anti-PD-L1 therapy for liver tumors in the presence of TREM-1+ TAMs remain obscure. Because TREM-1+ TAMs are closely associated with tumor microenvironment, their potential interplays with other TILs in hypoxic tumor environment require further investigation to enrich our knowledge about TREM-1+ TAMs behavior in HCC.

In this work, we found that hypoxic tumor environment modulated TREM-1 expression in TAMs,

ARTICLE INFORMATION:

From the [1]Division of Hepatobiliary and Pancreatic Surgery, Department of Surgery, The First Affiliated Hospital, School of Medicine, Zhejiang University, Hangzhou, China; [2]NHFPC Key Laboratory of Combined Multi-organ Transplantation, Hangzhou, China; [3]Key Laboratory of the Diagnosis and Treatment of Organ Transplantation, CAMS, Hangzhou, China; [4]Key Laboratory of Organ Transplantation, Zhejiang Province, Hangzhou, China; [5]Collaborative Innovation Center for Diagnosis Treatment of Infectious Diseases, Hangzhou, China; [6]Department of Hepatobiliary and Pancreatic Surgery, Taihe Hospital, Hubei University of Medicine, Hubei, China.

ADDRESS CORRESPONDENCE AND REPRINT REQUESTS TO:

Shusen Zheng, M.D., Ph.D.
Division of Hepatobiliary and Pancreatic Surgery
Department of Surgery, First Affiliated Hospital
School of Medicine, Zhejiang University
No. 79 Qing chun Road
Hangzhou 310003, China
E-mail: shusenzheng@zju.edu.cn
Tel.: +1-86-571-87236466
or

Lin Zhou, M.D., Ph.D.
Division of Hepatobiliary and Pancreatic Surgery
Department of Surgery, First Affiliated Hospital
School of Medicine, Zhejiang University
No. 79 Qing chun Road
Hangzhou 310003, China
E-mail: zhoulin99@zju.edu.cn
Tel.: +1-86-571-87236466

resulting in immunosuppression dependent on recruitment of Foxp3^{+} Tregs by chemokine (C-C motif) ligand 20 (CCL20) up-regulation in HCC. First, TREM-1^{+} TAMs were observed to be abundant within HCC tissue with high expression of HIF-1α, which was capable of directly up-regulating TREM-1 level in TAMs *in vitro*. Then, in tumor-bearing models, TREM-1^{+} TAMs exhibited the ability to induce immunosuppression related to dysfunction and apoptosis of CD8^{+} T cells. Although PD-L1 expression was high in TREM-1^{+} TAMs, PD-L1 blockade failed to improve TREM-1^{+} TAM-mediated immunosuppression in tumor-bearing mice. Intriguingly, high CCL20 expression was induced in hypoxic TREM-1^{+} TAMs through ERK/NF-κβ pathway activation and was responsible for the recruitment of CCR6^{+} Tregs. Blocking TREM-1 signaling with the inhibitor GF9 significantly attenuated CD8^{+} T cell dysfunction and abrogated the resistance to PD-L1 blockade. These results suggested that TREM-1^{+} TAMs are candidates to target to improve anti-PD-L1 therapeutic efficacy in HCC.

Materials and Methods

SPECIMENS AND BIOCHEMICAL REGENTS

A total of 119 tissue samples were obtained from patients who underwent hepatocellular carcinoma curative resection between 2012 and 2014 in the First Affiliated Hospital of Zhejiang University, School of Medicine. These tissues were subjected to tissue microarray, immunohistochemistry, immunofluorescence, and survival analysis. Written informed consent was obtained from each participant. This project was approved by the Ethics Committee of First Affiliated Hospital of Zhejiang University, School of Medicine, and clinical data of all subjects were summarized in Supporting Table S1.

1,4-diamino-2,3-dicyano-1,4-bis(2-aminophenylthio)butadiene (U0126) and caffeic acid phenethyl ester (CAPE), the inhibitor of ERK and NF-κβ signal, respectively, were purchased from Selleck Chemicals (Houston, TX). The ligand-independent peptide-based TREM-1 inhibitor GF9 (the TREM-1$_{213-221}$, GLLSKSLVF), control peptide (GLLSGSLVF), and TREM-1 antagonist LP17 (LQVTDSGLYRCVIYHPP) were synthesized by HuaBio. Inc. (Shanghai, China).

CELL CULTURE AND HYPOXIA TREATMENT

The methods of cell culture and transfection are shown in Supporting Information.

For hypoxia treatment, bone marrow–derived macrophages (BMDMs) were exposed to hypoxia environment (1% O_2, 5% CO_2, 94% N_2) in a hypoxic incubator (Thermo Scientific, Waltham, MA) for an indicated time. Condition medium (CM) consisted of complete medium and hepa1-6 supernatant (with the ratio of 1:1) after incubation under hypoxia, and was used to mimic the hypoxic tumor environment.

DUAL-LUCIFERASE REPORTER SYSTEM ASSAYS

The procedure of Dual-Luciferase Reporter System assays is described in detail in Supporting Information.

MOUSE TUMOR MODELS AND TREATMENT

Mouse tumor model establishment and drug treatment experiments are described in detail in Supporting Information.

FLOW CYTOMETRY AND CHEMOKINES DETECTION

Mice were sacrificed at indicated times after tumor inoculation. The left liver lobes with tumor lesions were harvested and minced to prepare single cell suspension. The mononuclear cells isolated from liver tumors through OptiPrep Density Gradient Medium (Sigma-Aldrich, St. Louis, MO) were applied to multicolor flow cytometry (Canto II; BD, China). T cells were enriched by Magnetic Particles (551516; BD, PMG, San Diego, CA). CD8^{+} T-cells apoptosis was detected by annexin V APC/7-AAD apoptosis kit (Multiscience, Hangzhou, China) according to manufacturer's instructions. The detail of staining procedures and chemokines detection are described in Supporting Information.

CHEMOTAXIS ASSAY

Chemotaxis assay was conducted using 6-µm transwell filter (Corning Costar, Cambridge, MA) and repeated at least three times. Lymphocytes were isolated from peripheral blood of subcutaneous tumor–bearing model mouse and were equalized into top chamber. After 6 hours, the suspension from bottom chamber was collected and the $CD4^+CD25^+Foxp3^+$Tregs were enumerated by flow cytometry.[18]

IMMUNOHISTOCHEMISTRY, IMMUNOFLUORESCENT AND IMMUNOBLOTTING ASSAY

The 3-µm slides were used for immunohistochemistry (IHC) or immunofluorescent staining, and the images were evaluated by two independent pathologists. IHC scoring criteria is shown in Supporting Fig. S1A. Procedures of immunoblotting and immunohistochemistry are detailed in Supporting Information.

QUANTITATIVE RT-PCR

After total RNA extraction and reverse transcription in complementary DNA, real-time quantitative PCR was performed using the SYBR Premix Ex Taq II (TaKaRa, Tokyo, Japan) according to the manufacturer's instruction. The threshold cycle value was used to analyze the gene expression among the different groups. Independent experiment was repeated at least three times. Primers are shown in Supporting Table S2.

STATISTICAL ANALYSIS

Statistical analysis was performed using GraphPad Prism 5 software (La Jolla, CA). Pearson correlation and regression analysis were used to assess the relationship between TREM-1+ TAMs number and apoptosis number, TREM-1+ TAMs number and CD8+ T cells number, CD8+ T cells number and Foxp3+Tregs number, and Foxp3+Tregs number and TREM-1+ TAMs number within human HCC tissue. Flow cytometry data were analyzed by FlowJo.10 (TreeStar, Ashland, OR). Student two-tailed t test was used for comparison of quantitative data from different groups. Kaplan-Meier survival curves were plotted and were compared by log-rank test. $P < 0.05$ was considered statistically significant. (*$P < 0.05$; **$P < 0.01$; ***$P < 0.001$; ****$P < 0.0001$.)

Results

TREM-1+ TAMS ARE ABUNDANT WITHIN HYPOXIC TISSUE AND CORRELATE WITH POOR PROGNOSIS

TREM-1+ TAMs have been found in different kinds of tumors.[19] However, it is unclear how TREM-1+ TAMs behave within HCC with a hypoxic environment. Here, we demonstrated that TREM-1+ TAMs are abundant within tumor tissue with high expression of HIF-1α (Fig. 1A,B; Supporting Fig. S1A), which was closely associated with advanced stages and a poor prognosis (Supporting Fig. S1B). In addition, the number of TREM-1+ TAMs was significantly increased in HCC in advanced stages, suggesting abundant TREM-1+ TAMs are involved in malignant progression (Supporting Fig. S1C). Although tumor infiltration by CD8+ T cells is associated with a more favorable prognosis,[20,21] CD8+ T cells were inclined to infiltrate into HCC with an abundance of TREM-1+ TAMs and then undergo apoptosis (Fig. 1C); thus, tumor-infiltrating CD8+ T cells could not improve overall survival and disease-free survival of HCC (Fig. 1D). This observation was further supported by the analysis of online data from the Tumor Immune Estimation Resource (Supporting Fig. S1D).[22] Therefore, patients with HCC do not benefit from infiltration of CD8+ T cells, probably because of CD8+ T cell apoptosis and dysfunction, which could be mediated by TAMs.[23] Moreover, the presence of abundant TREM-1+ TAMs indicated a poor prognosis (Fig. 1E). Thus, TREM-1+ TAMs contributed to the poor prognosis of HCC, likely by suppressing CD8+ T-cell functions, albeit with upward trend of CD8+ T-cells infiltration.

HIF-1α-INDUCED TREM-1+ TAMs CONTRIBUTE TO THE DYSFUNCTION OF CD8+ T CELLS AND HCC PROGRESSION

Adequate evidence has shown that TAMs are subjected to hypoxia.[5] Here, the impact of hypoxia on TAMs was validated by showing the up-regulation of HIF-1α expression along with the increasing expression of TREM-1 by immunohistochemistry and immunofluorescent staining (Supporting
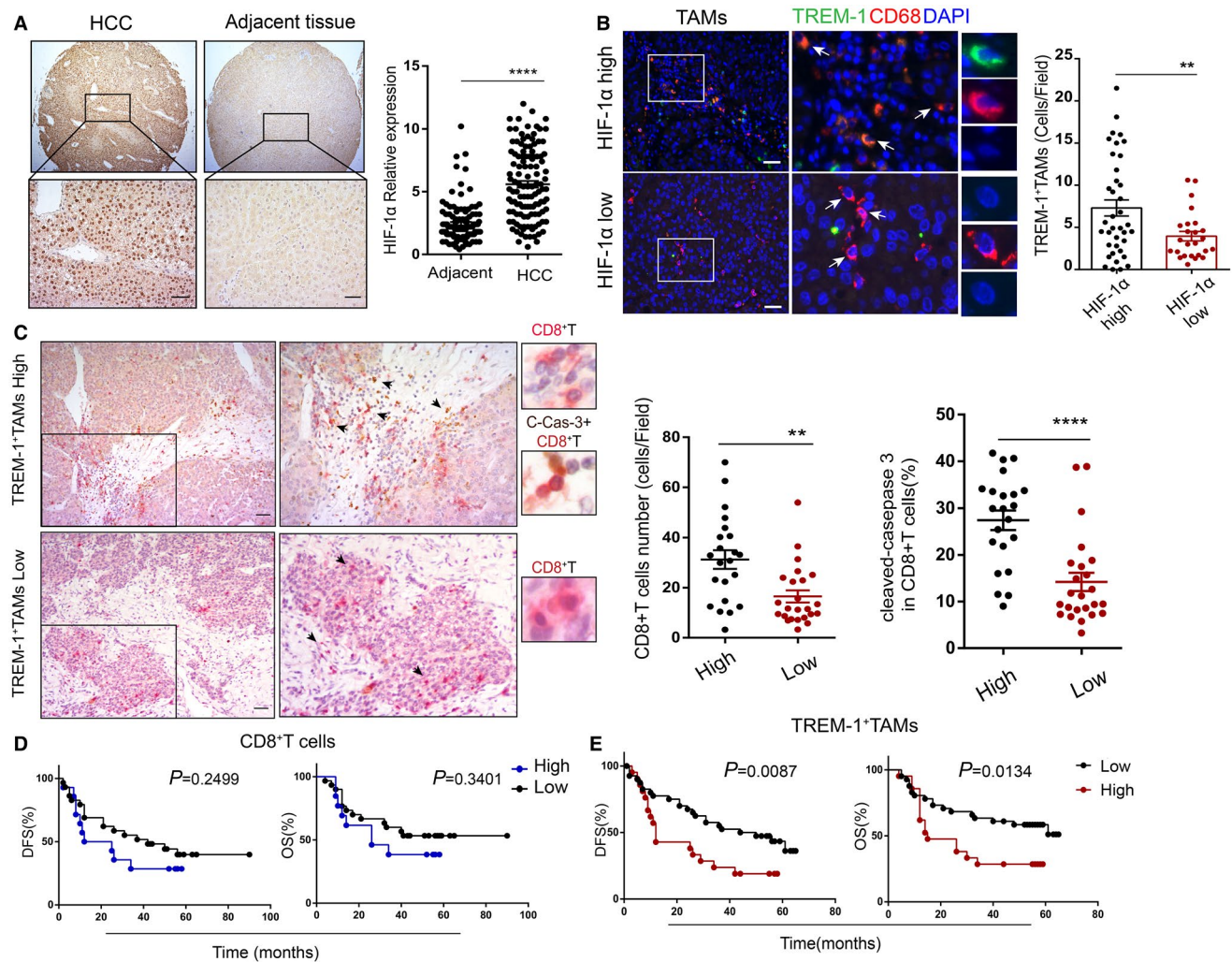
FIG. 1. TREM-1$^+$ TAMs within HIF-1α expression tumor tissues indicate poor prognosis of HCC. (A) Immunohistochemical staining of HIF-1α in HCC tissue array (left panel, magnification of ×40 on top and ×200 for bottom), and comparison of relative HIF-1α expression between tumor and adjacent tissues according to immunohistochemical staining score. Data are presented as mean ± SEM (right panel, n = 119). (B) Representative images of immunofluorescent staining with CD68 (red), TREM-1 (green) and DAPI (blue) within HCC tissues with high and low expression of HIF-1α, referred to as immunohistochemical staining score ≥6 and <6, respectively (left panel, arrows indicate TREM-1$^+$CD68$^+$ TAMs on top and TREM-1$^-$CD68$^+$ TAMs on bottom; magnification, ×400), and comparison of average number of TREM-1$^+$ TAMs within 10 random fields of ×200 magnification between HCC tissues with high (n = 38) and low (n = 25) expression of HIF-1α. Magnification, ×400. Data are shown as mean ± SEM. (C) Left panel, costaining with CD8 (red) and C-Cas-3 (brown) within HCC tissues with high or low TRME-1$^+$ TAMs, indicating that the number of TRME-1$^+$ TAMs per field was ≥6 and <6, respectively. Magnification, ×100. Right panel, the average number of CD8$^+$ T cells and percentage of C-Cas-3 in CD8$^+$ T cells within 10 random fields of ×200 magnification were compared between HCC tissues with high (n = 22) and low (n = 24) TRME-1$^+$ TAMs. Data are presented as mean ± SEM. (D) Comparison of overall survival and disease-free survival curves between patients with HCC with high (n = 14) and low CD8$^+$ T cells (n = 29), indicating the number of CD8$^+$ T cells per field from high magnification was ≥30 and <30, respectively ($P > 0.05$), and (E) between patients with HCC with high (n = 38) and low (n = 25) TREM-1$^+$ TAMs ($P < 0.05$). *$P < 0.05$; **$P < 0.01$; ***$P < 0.001$; ****$P < 0.0001$. Abbreviations: C-Cas-3, cleaved-caspase-3; DAPI, 4′,6-diamidino-2-phenylindole.

Fig. S1E). These results suggested that TREM-1$^+$ TAMs were present within the hypoxic HCC environment. *In vitro*, the level of TREM-1 but not that of TREM-2 significantly increased in BMDMs (F4/80$^+$ CD11b$^+$) after culture under hypoxic conditions for the indicated time (Supporting Fig. S1F),

and the up-regulation of TREM-1 expression mainly relied on hypoxia rather than tumor-derived CM (Supporting Fig. S2A). Additionally, we investigated whether TREM-1^{+} TAMs accumulation was associated with tumor progression *in vivo*. It is clear that the rapid growth of solid tumors contributes to the hypoxic environment and elevates the expression of HIFs.[1,24] In accordance, the HIF-1α level gradually increased during tumor growth in an orthotopic liver tumor model (Fig. 2A), and CD16/32[+]TREM-1^{+} TAMs gradually accumulated within the tumor tissue

as well (Fig. 2B). We next sought to investigate the mechanism by which HIF-1α regulates TREM-1 expression and the roles of TREM-1^{+} TAMs in HCC progression. HIF-1α is implicated in the transcription of various genes through binding to hypoxia response elements (HREs),[25] and exogenous augmentation of the HIF-1α was found to markedly up-regulate TREM-1 expression in BMDMs (Supporting Fig. S2B). The results of a Dual-Luciferase Reporter System assay determined the specific HREs within the promoter region of TREM-1. Specifically, the
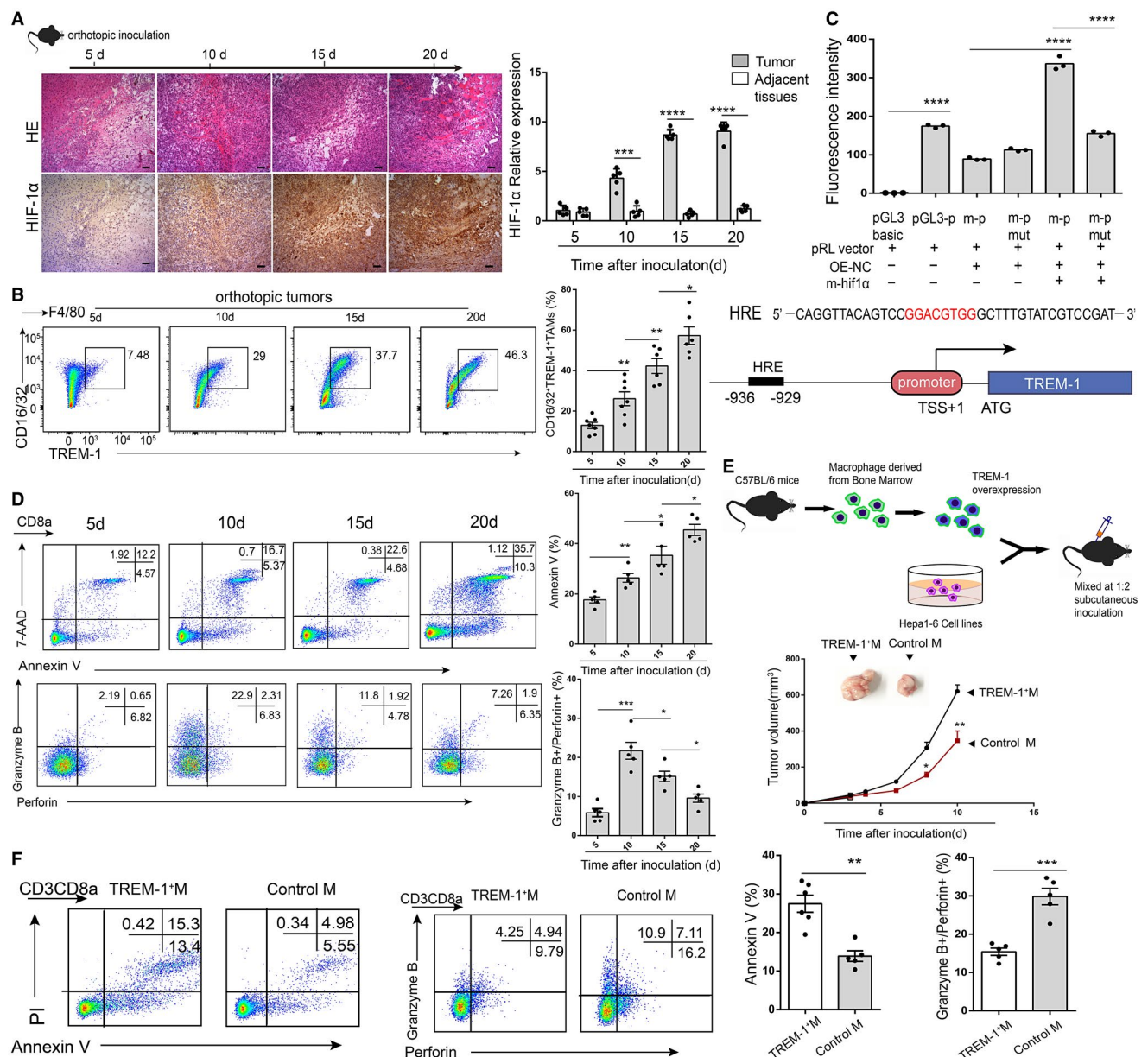
FIG. 2. TREM-1⁺ TAMs are induced by tumor hypoxic environment and exhibit immunosuppressive effect. (A) HE staining and immunohistochemical staining with HIF-1α in tumor tissues after orthotopic inoculation for indicated time (left panel), and quantification of relative HIF-1α expression according to immunohistochemical staining (right panel, n = 5 for each group). Magnification, ×100. Data are presented as mean ± SEM. (B) Macrophages were isolated from tumor tissues after orthotopic inoculation for indicated time and labelled with F4/80, CD16/32, and TREM-1 for analysis of flow cytometry. Percentage of CD16/32⁺TREM-1⁺ TAMs population are presented as mean ± SEM (n ≥ 6 for each group). (C) Dual-luciferase reporter for TREM-1 and HIF-1α, and the HIF-1α binding sequence within promoter of HIF-1α was -936~-929 (GGACGTGG). (D) CD8⁺ T cells were isolated and enriched from tumor tissues after inoculation for indicated time and then labelled with CD8a, granzyme B, perforin, and 7-AAD, annexin V for analyzing cytotoxic function and apoptosis of CD8⁺ T cells by flow cytometry. The percentage of annexin V and granzyme B⁺/perforin⁺ population of CD8⁺ T cells were shown as mean ± SEM (n = 5 for each group). (E) Schematic illustration of establishment of tumor model within C57BL/6 mice through subcutaneous inoculation of mixture of Hepa1-6 cells and macrophages (at ratio of 2:1) with or without TREM-1 overexpression (upper panel, indicated as TREM-1⁺ M and Control M, respectively). Tumor growth was monitored regularly, and tumor volume shown are mean ± SD (lower panel, n = 6 for each group). (F) CD8⁺ T cells were isolated and enriched from tumor tissues in TREM-1⁺ M or Control M groups at indicated timepoint and then labelled with CD3, CD8a, granzyme B, perforin, and PI, annexin V for analyzing cytotoxic function and apoptosis of CD8⁺ T cells by flow cytometry. The percentage of apoptosis (indicated as annexin V percentage) and granzyme B⁺/perforin⁺ population of CD8⁺ T cells are shown as mean ± SD (n = 5 for each group). *$P < 0.05$; **$P < 0.01$; ***$P < 0.001$; ****$P < 0.0001$. Abbreviations: 7-AAD, 7-amino-actinomycin D; PI, propidium iodide.

sequence GGACGTGG (-936~-929 bp) bound with HIF-1α, leading to the transcriptional up-regulation of TREM-1 (Fig. 2C). Furthermore, tumor growth was accompanied by CD8⁺ T-cell apoptosis and dysfunction, characterized by reductions in the perforin and granzyme B (Fig. 2D). To investigate whether this immunosuppression was induced by TREM-1⁺ TAMs, hepa1-6 cells plus TREM-1⁺BMDMs (TREM-1⁺ M) or control BMDMs (Control M) was used to establish tumor-bearing model (Fig. 2E). In this model, a significant increase in the TREM-1 level was confirmed in the BMDMs with TREM-1 overexpression by flow cytometry (Supporting Fig. S2C). Intriguingly, TREM-1⁺ M significantly accelerated tumor growth and promoted CD8⁺ T-cell apoptosis and dysfunction (Fig. 2F).

TREM-1⁺ TAMs HAVE A HIGH LEVEL OF PD-L1 AND FACILITATE CD8⁺ T-CELL EXHAUSTION, A PROCESS THAT COULD NOT BE REVERSED BY PD-L1 BLOCKADE

Based on the above phenomena, we continued to explore the mechanism of TREM-1⁺ TAM-mediated CD8⁺ T-cell dysfunction. Given that PD-L1, a member of the B7 family, can respond to hypoxia,[26,27] the mRNA expression of B7-H4, PD-L1, B7-1, and B7-2 was compared between BMDMs treated by hypoxia

with or without CM, which was used to mimic the hypoxic tumor environment. We found that only the PD-L1 mRNA levels were strikingly elevated in the BMDMs after cotreatment with hypoxia and CM, suggesting that PD-L1 expression up-regulation was dependent on the coexistence of hypoxia and tumor metabolites (Fig. 3A). The small interfering RNA (siRNA)-mediated inhibition of TREM-1 was able to suppress PD-L1 expression in BMDMs under hypoxia conditions treated with CM, suggesting that PD-L1 expression up-regulation in BMDMs is partially reliant on TREM-1 (Fig. 3B). The high level of PD-L1 in TRME-1⁺ TAMs from the orthotopic liver tumor model suggested that TRME-1⁺ TAMs possess the potential to mediate immunosuppression through the programmed cell death 1 (PD-1)/PD-L1 axis (Fig. 3C). A high level of PD-L1 has been recognized as a powerful suppressor that supports tumor immune escape, and can efficiently respond to PD-L1 blockade therapy.[28] Although the PD-L1 expression up-regulation in TREM-1⁺ TAMs conferred the possibility of immunosuppression, the *in vivo* antitumor efficacy of PD-L1 blockade was abrogated in the TRME-1⁺ M group, which was characterized by an abundance of TREM-1⁺ TAMs (Fig. 3D; Supporting Fig. S2D). Specifically, TREM-1⁺ TAMs could effectively suppress CD8⁺ T-cell functions. Moreover, the functions of CD8⁺ T cells were suppressed in the TRME-1⁺ M group but significantly improved in the Control M group after PD-L1 blockade treatment (Fig. 3E).
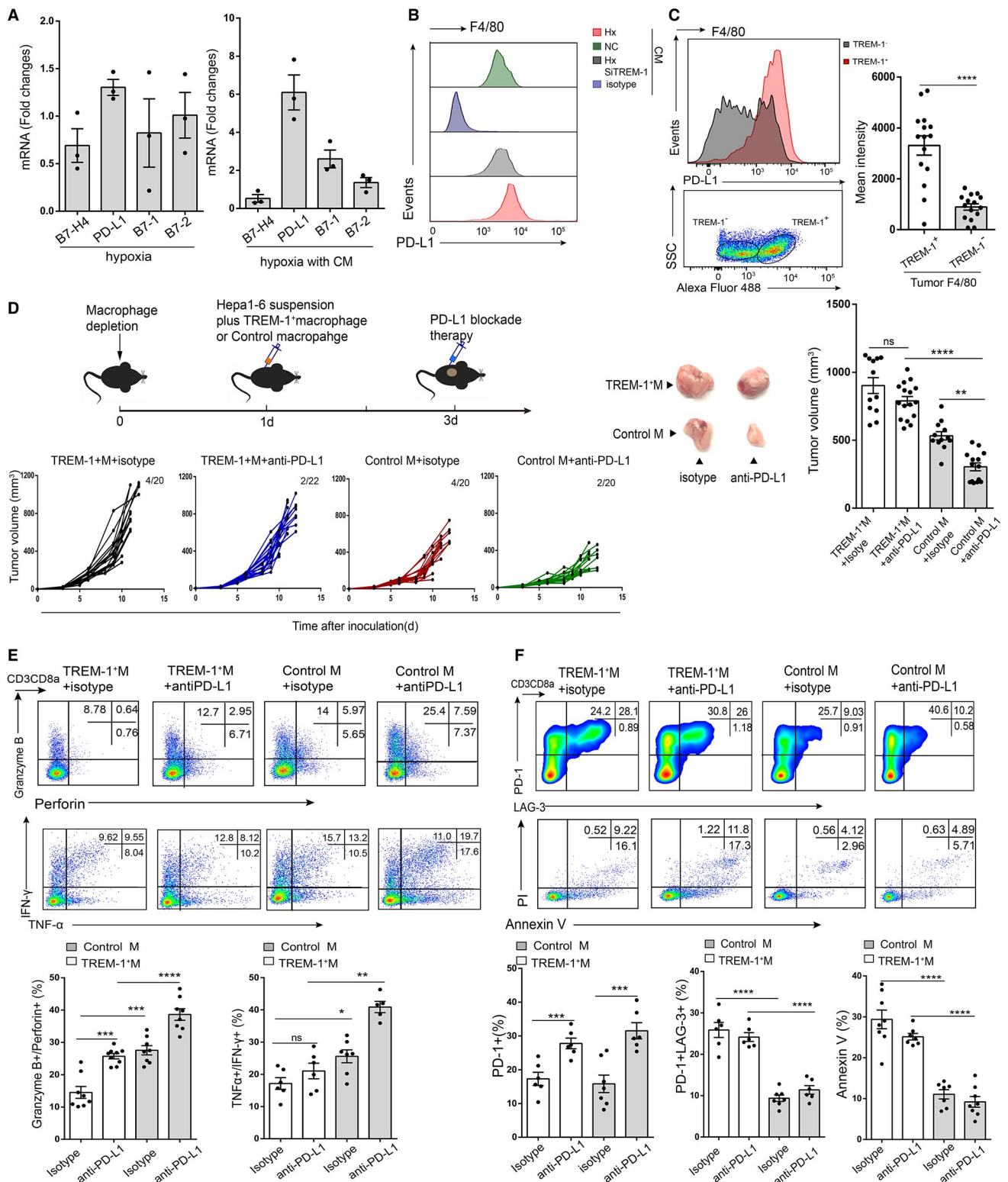
These results suggested that mice with an abundance of TREM-1$^+$ M hardly benefit from PD-L1 blockade treatment. PD-1 is a typical marker of effector T lymphocytes. Nevertheless, T cells with coexpression of PD-1 and LAG-3 represent an exhausted subset with function loss.[29,30] In line with the report by

FIG. 3. TREM-1^{+} TAMs confer resistance to anti-PD-L1 treatment in HCC. (A) Fold change of mRNA expression of B7-H4, PD-L1, B7-1, and B7-2 expressed within BMDMs after treated with hypoxia or combination of hypoxia and CM for 24 hours. Each individual point represents one experiment with triplicate. Data are presented as mean ± SEM. (B) PD-L1 expression in BMDMs with TREM-1 knockdown by siRNA was measured by flow cytometry with Hx and CM. (C) Amount of PD-L1 within isolated TAMs from orthotopic tumor tissues by flow cytometry (left panel), and subsequently being quantified and compared between group TREM-1^{+} and TREM-1^{-} based on mean PD-L1 expression intensity (right panel). Data are shown as mean ± SEM (n = 15 for each group). (D) Schematic illustration of anti-PD-L1 antibody treatment (20 mg/kg intraperitoneally on day 3, 6, and 9) for tumor lesions originated from subcutaneous inoculation of hepa1-6 cells plus TREM-1^{+} M or Control M (at ratio of 2:1) within C57BL/6, which were pretreated with neutral clodronate liposomes for 1 day (left upper panel), and followed by assessment of tumor growth (left lower panel, n = 20, 22, 20, and 20 and number of accidental deaths was 4, 2, 4, and 2 in groups from left to right, respectively, shown in right top), appearance of tumor lesion (middle panel), comparison of tumor volume (right panel, n ≥ 10 for each group), and (E) detection of cytotoxic function (labelled with granzyme B and perforin, or IFN-γ and TNF-α), (F) exhausted status (labelled with PD-1 and LAG-3) and apoptosis (labelled with PI and annexin V) of CD8^{+} T cells (labelled with CD3 and CD8). Percentage of granzyme B^{+}/perforin^{+} papulation and TNF-α^{+} and IFN-γ^{+} population (E), and PD-L1^{+} population, PD-L1^{+}LAG-3^{+} population, and annexin V^{+} population (F) of CD8^{+} T cells are presented as mean ± SEM, $n ≥ 6$ for each group, and each dot represented a sample of CD8^{+} T cells isolated from two individual tumors (E, F). *$P < 0.05$; **$P < 0.01$; ***$P < 0.001$; ****$P < 0.0001$. Abbreviations: Hx, hypoxia; IFN-γ, interferon-γ.

Tumeh et al.,[31] we found that PD-L1 blockade was able to increase the percentage of PD-1^{+} cells in CD8^{+} T-cell population but unable to prevent CD8^{+} T cells from undergoing exhaustion and apoptosis in the presence of TREM-1^{+} TAMs (Fig. 3F). CD8^{+} T-cells exhaustion and apoptosis were significantly lower in the Control M group than in the TREM-1^{+} M group. Therefore, anti-PD-L1 treatment in the Control M group displayed powerful antitumor efficacy. Our results demonstrated that TREM-1^{+} TAMs endowed HCC with resistance to anti-PD-L1 therapy and the ability to induce CD8^{+} T-cells exhaustion, implying that a pathway, not the PD-L1/PD-1 axis, played a substantial role in the process by which TREM-1^{+} TAMs induced CD8^{+} T-cells exhaustion in HCC.

TREM-1^{+} TAMs ARE CRITICAL FOR Foxp3^{+} Treg ACCUMULATION, AND Treg DEPLETION COULD ABROGATE THE EXHAUSTION OF CD8^{+} T CELLS

In addition to the PD-1/PD-L1 checkpoint molecules, CD4^{+}CD25^{+}Foxp3^{+} Tregs have been determined to be another canonical factor that impairs CD8^{+} T-cell functions,[32,33] and natural regulatory T cells can be recruited into the tumor microenvironment by various chemokines secreted by TAMs.[7] To explore whether the TREM-1^{+} TAM-associated PD-L1 resistance was derived from Treg infiltration, the percentage of CD4^{+}CD25^{+}Foxp3^{+} Tregs was detected in the tumor. Predominantly, CD4^{+}CD25^{+}Foxp3^{+} Treg infiltration was elevated

in the TREM-1^{+} M group regardless of whether the mice were treated with anti-PD-L1 antibody (Fig. 4A). In accordance, a large number of Foxp3^{+} Tregs were observed to accumulate within tumor zone of CD8^{+} T-cell infiltration, and particularly around CD8^{+} T cells by immunofluorescent staining. Meanwhile, there was a positive correlation among the number of Foxp3^{+} Tregs, the number of TREM-1^{+} TAMs, and the number of CD8^{+} T cells within HCC tissue (Fig. 4B). Thus, TREM-1^{+} TAM-derived immunosuppression seemed to act through Foxp3^{+} Treg recruitment.

Next, the impacts of TREM-1^{+} TAM-associated Tregs on CD8^{+} T-cell exhaustion and anti-PD-L1 resistance were investigated. First, tumor growth could be delayed after Treg depletion by anti-CD25 antibody albeit the abundance of TREM-1^{+} TAMs. In addition, PD-L1 blockade-induced inhibition of tumor growth was dramatically enhanced by combining the treatment with anti-CD25 antibody (Fig. 4C,D). In addition, Tregs within the tumor tissue were effectively depleted by anti-CD25 antibody, resulting in improved cytotoxic functions and inhibited exhaustion in CD8^{+} T cells, and enhanced anti-PD-L1 efficacy (Fig. 4E,F; Supporting Fig. S2E), suggesting that Treg infiltration was a key contributor to TREM-1^{+} TAM-associated anti-PD-L1 resistance. However, anti-CD25 treatment can evoke various autoimmune diseases, due to the extensive depletion of Tregs.[34] Therefore, the rational management of Tregs is likely to benefit from exploring the mechanism by which TREM-1^{+} TAMs regulate Treg trafficking in HCC.
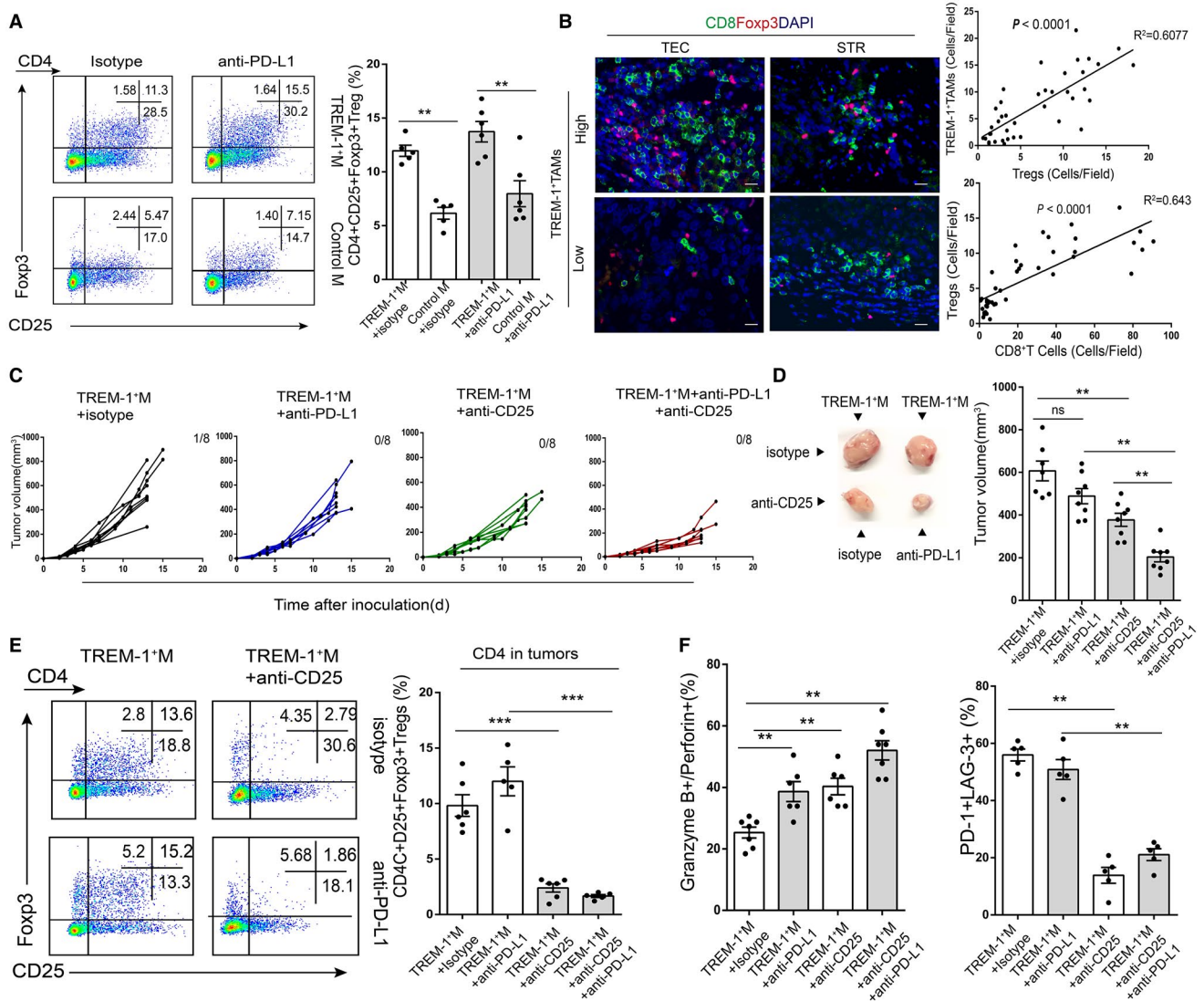
FIG. 4. TREM-1^{+} TAMs facilitate immunosuppression and anti-PD-L1 resistance by recruiting CD4^{+}CD25^{+}Foxp3^{+} Tregs in HCC. (A) Analysis of percentage of CD4^{+}CD25^{+}Foxp3^{+} Tregs population within tumor lesions harvested from hepa1-6 generating tumor (same as model described in Fig. 3D) by flow cytometry. Data are shown as mean ± SEM (n = 5 or 6). (B) Representative immunofluorescent images stained with CD8 (green), Foxp3 (red), and DAPI (blue) within TEC and STR tissues from patients with HCC with high or low TRME-1^{+} TAMs (left panel). Magnification, ×640. Correlation of the number of Foxp3^{+} Tregs to the number of TREM-1^{+} TAMs (n = 40) and the number of CD8^{+} T cells (n = 42) were analyzed by Pearson analysis. (C-F) The mixture of heap1-6 cells plus TREM-1^{+} M (at ratio of 2:1) was subcutaneously inoculated within C57BL/6 mice pretreated with neutral clodronate liposomes for 1 day, followed by treatment of anti-CD25 antibody (25 mg/kg intraperitoneally) on day 1 and 7 as well as treatment of anti-PD-L1 antibody (20 mg/kg intraperitoneally) on day 3, 6, and 9 after inoculation. Tumor growth was examined (C, n = 8 for each group, and number of accidental deaths was 1, 0, 0, and 0 in groups from left to right, respectively, shown in top right). Tumor appearance (D, left panel) and volume (D, right panel) were compared among different groups (n = 7 or 8). All tumor lesions were harvested for analyzing percentage of CD4^{+}CD25^{+}Foxp3^{+} Tregs population (E, n = 5 or 6), and granzyme B^{+}/perforin^{+} papulation and PD-L1^{+}LAG-3^{+} population (F, n = 6 or 7) of CD8^{+} T cells. Data are shown as mean ± SEM. *$P < 0.05$; **$P < 0.01$; ***$P < 0.001$; ****$P < 0.0001$. Abbreviations: DAPI, 4′,6-diamidino-2-phenylindole; STR, stroma; TEC, tumor epithelial cells.

TREM-1 UP-REGULATES CCL20 THROUGH ERK/NF-κβ PATHWAY, AND TREM-1⁺ TAMs RECRUIT Foxp3⁺ Tregs DEPENDENT ON THE CCL20/CCR6 AXIS WITHIN HYPOXIC TUMOR ENVIRONMENT

TREM-1 is an important proinflammation receptor that can regulate various chemokines.[35] In agreement with this function, the levels of multiple chemokines were altered by CRISPR-cas9-mediated TREM-1 knockdown in BMDMs under hypoxic tumor conditions according to the analysis of chemokine array (Supporting Fig. S2F). Noticeably, Treg-associated chemokines, including CCL5, CCL20, CCL17, and CCL22, were decreased by TREM-1 knockdown (Supporting Fig. S3A), suggesting that TREM-1 potentially recruits Tregs into tumors and that Tregs tend to be abundant within tumors with presence of TREM-1⁺ TAMs. However, CCL20 was up-regulated, whereas the levels of CCL5 and CCL22 were reduced in BMDMs after cotreatment with hypoxia and CM, as measured by both chemokine array and flow cytometry (Fig. 5A,B; Supporting Fig. S3B). CCR6, the only currently identified receptor of CCL20,[36] was widely expressed on Tregs in tumors (Supporting Fig. S3C). In addition, the CCR6⁺ Tregs accounted for the main part of Tregs, and the percentage of CCR6⁺ Tregs significantly increased as tumor growth increased (Supporting Fig. S3D). These data indicated that CCL20 could be stably elevated in hypoxic tumor environment and played a predominant role to attract Tregs into tumors. Notably, a high level of CCL20 was detected in both TREM-1⁺ TAMs and TREM-1⁺ BMDMs (Supporting Fig. S3E), indicating that TREM-1 probably increases CCL20 expression in macrophages under hypoxic tumor environment. MAPK pathway is involved in up-regulation of the expression of various chemokines and is often activated in macrophages under hypoxia.[37,38] Accordingly, the amounts of phosphorylated ERK and p65, both of which indicate the activation of MAPK pathway, were increased within BMDMs treated with hypoxia (Fig. 5C). However, the protein levels of phosphorylated ERK and p65 were significantly inhibited by siRNA-mediated TREM-1 knockdown or slightly reduced by the TREM-1 antagonist LP17 despite the presence of hypoxia (Fig. 5C; Supporting Fig. S3F). Predominantly, TREM-1 knockdown inhibited p65

nuclear translocation in a hypoxic environment (Supporting Fig. S4A). Additionally, the exogenous overexpression of TREM-1 was able to facilitate ERK phosphorylation in aid of p65 nuclear localization in BMDMs treated with CM, and this phenomenon could be reversed by ERK inhibitor U0126 (Fig. 5D). These results suggested that hypoxia-associated ERK activation relies on TREM-1 up-regulation, which in turn activates the NF-κβ pathway within tumor environment. The key molecular event is p65 nuclear translocation through ERK/NF-κβ pathway. Moreover, NF-κβ inhibitor CAPE abolished the up-regulation of CCL20 mediated by exogenous overexpression of TREM-1 in BMDMs (Fig. 5E), suggesting that TREM-1 up-regulates CCL20 through the ERK/NF-κβ pathway.

In vitro chemotaxis assay demonstrated that TREM-1⁺ BMDMs cultured with CM could attract more CD4⁺CD25⁺Foxp3⁺ Tregs and this process was blocked with anti-CCL20 neutralizing antibody (Supporting Fig. S4B), which provided a potential strategy to reduce Tregs trafficking. *In vivo*, treatment with anti-CCL20 neutralization antibody remarkably reduced the infiltration of Foxp3⁺ Tregs, especially CCR6⁺Foxp3⁺ Tregs, and delayed tumor growth in orthotopic liver tumor model (Supporting Fig. S4C,D). Furthermore, an increase in the percentage of tumor-infiltration CD8⁺ T cells after anti-CCL20 treatment was examined (Supporting Fig. S4E). In line with these results, CCL20 blockade contributed to the intratumoral infiltration of CD8⁺ T cells, as measured by immunofluorescent staining (Supporting Fig. S4F). Intriguingly, anti-CCL20 could significantly enhance antitumor efficacy of PD-L1 blockade in subcutaneous tumor model (Fig. 5F). Overall, the up-regulation of CCL20 in TREM-1⁺ TAMs was able to recruit CD4⁺CD25⁺CCR6⁺Foxp3⁺ Tregs through a process dependent on ERK/NF-κβ pathway activation, and the CCL20 blockade could abrogate anti-PD-L1 resistance in HCC.

TREM-1 INHIBITOR GF9 ABROGATES IMMUNOSUPPRESSION AND PD-L1 BLOCKADE RESISTANCE

Our data thus far suggest that TREM-1⁺ TAMs induced by hypoxic tumor environment recruit CCR6⁺Foxp3⁺ Treg to promote immunosuppression.
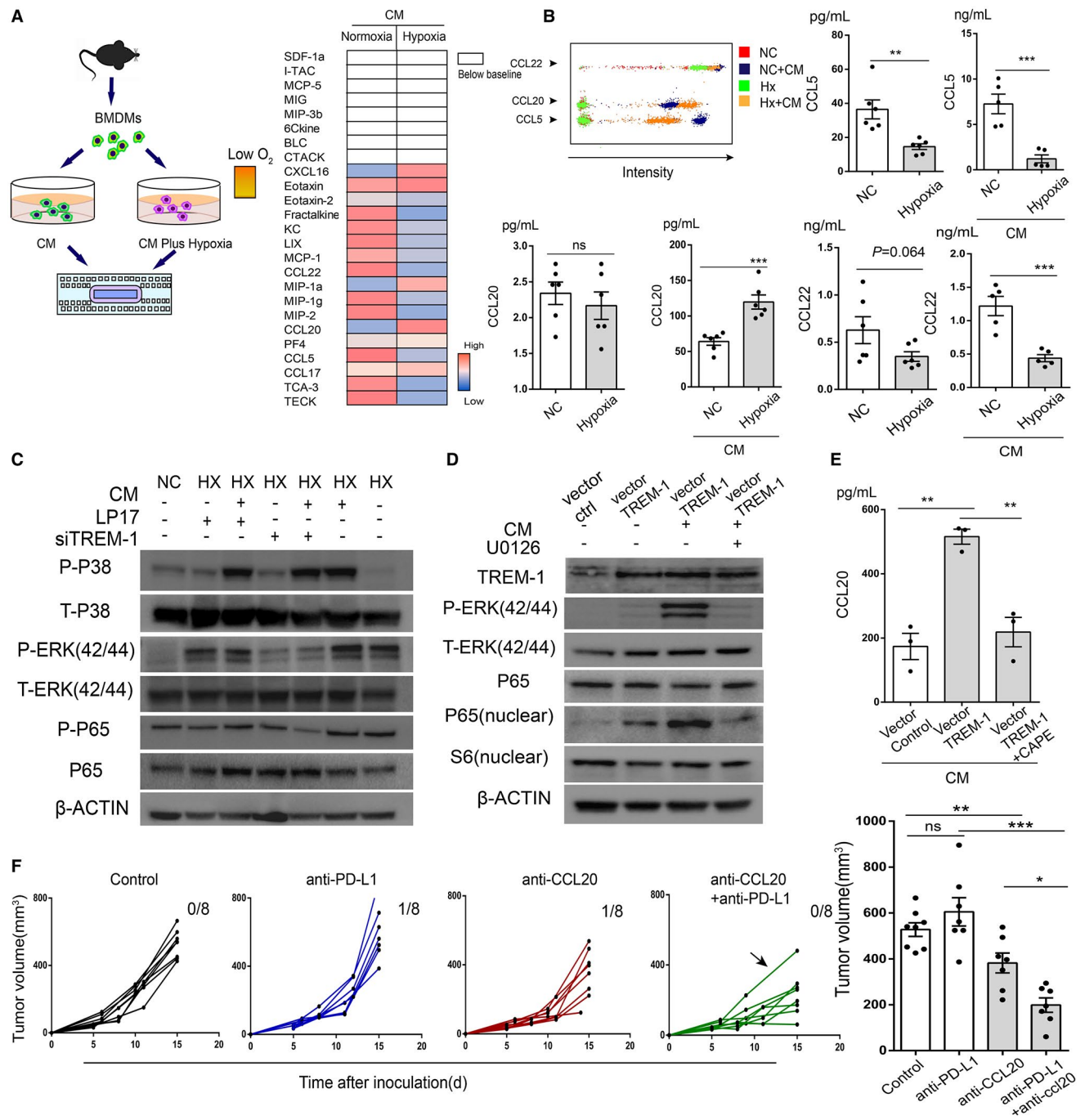
To confirm whether TREM-1 signaling blockade could reverse this immunosuppression, we synthesized the ligand-independent TREM-1 inhibitor GF9, which can specifically inhibit the TREM-1 pathway,[39,40] and evaluated its efficacy in HCC. As shown in Fig. 6A,B, treatment with GF9 presented obvious inhibitory effects on tumor growth and improved mouse survival. Furthermore, GF9 treatment strikingly

reduced CCR6$^+$Foxp3$^+$ Tregs recruitment and apoptosis ratio of CD8$^+$ T cell and enhanced the cytotoxic function of CD8$^+$ T cell (Fig. 6C). In light of many limitations of anti-PD-L1 treatment for tumors,[41] we sought to explore the potential that TREM-1 blockade with GF9 could improve the antitumor efficacy of PD-L1 blockade treatment. The results showed that the combination of PD-L1 blockade

FIG. 5. TREM-1$^+$ TAMs attract Foxp3$^+$ Tregs through producing CCL20. (A) Schematic diagram of chemokines array for supernatant of BMDMs after treatment of CM with or without hypoxic condition for 24 hours (left panel), and difference in expression of chemokines secreted by BMDM treated with indicated conditions (right panel). (B) Amount of CCL5, CCL20, and CCL22 produced by BMDMs after treatment of CM with Hx or normoxia (NC) were detected by flow cytometry (n = 5). Data are shown as mean ± SEM. (C) Analysis of amount of proteins related to MAPK pathway and NF-κβ-p65 pathway immunoblotting within BMDMs with TREM-1 pathway blockage by siRNA (siTREM-1) or antagonist LP17 (20 ug/mL) after treatment of CM with hypoxic condition for 24 hours. NC was referred to as BMDMs treated under normoxia. (D) Amount of proteins related to ERK/ NF-κβ was measured by immunoblotting within BMDMs with overexpression of TREM-1 (indicated as vector-TREM-1, and empty vector was indicated as vector-ctrl) after treatment of CM with addition of ERK inhibitor U0126 for 24 hours. (E) Supernatant from culture of BMDMs with overexpression of TREM-1 under treatment of CM with or without addition of NF-κβ inhibitor CAPE for 24 hours was collected for detection of CCL20 amount by flow cytometry (n = 3); data are shown as mean ± SD. (F) The mixture of heap1-6 cells was subcutaneously inoculated within C57BL/6 mice, followed by treatment of anti-CCL20 antibody (0.5 mg/kg intravenously) on day 3, 6, 9, and 12 as well as treatment of anti-PD-L1 antibody (20 mg/kg intraperitoneally) on day 5, 8, 11, and 14 after inoculation. Tumor growth was monitored regularly (left panel, n = 8 for each group, and number of accidental deaths was 0, 1, 1, and 0 in groups from left to right, respectively, shown in top right), and the black arrow in anti-PD-L1+anti-CCL20 group indicated the tumor out of blockade CCL20 and PD-L1 effects. Tumor volume were compared among different groups (right panel, n = 6 or 8). Data are shown as mean ± SEM. *P < 0.05; **P < 0.01; ***P < 0.0001. Abbreviations: Hx, hypoxia; NC, negative control.

and GF9 treatment significantly attenuated tumor growth and improved mouse survival (Fig. 6D-F). Thus, these data demonstrated that GF9 treatment could abrogate TREM-1$^+$ TAM-mediated immunosuppressive effects and anti-PD-L1 resistance.

Discussion

Hypoxic environment is widely accepted as a barrier to antitumor therapy.[42] Although HIF-1α is frequently activated in response to hypoxia and determined to be involved in the immunosuppression, the exact regulatory process of hypoxia-induced immunosuppression remains largely unknown.[6] Here, we found that TAMs were educated by hypoxic tumor environment and highly expressed TREM-1 in an HIF-1α-dependent manner in HCC. Furthermore, the abundance of TREM-1$^+$ TAMs was associated with infiltration and apoptosis of CD8$^+$ T cells in HCC tissues. Although CD8$^+$ T-cell infiltration is beneficial for antitumor therapy, a variety of other leukocytes, some of which induce CD8$^+$ T-cell dysfunction, infiltrate solid tumors.[43] Therefore, our result that the infiltration of CD8$^+$ T cells did not improve prognosis in HCC was probably due to the dysfunction of CD8$^+$ T cells.

Next, we revealed that TREM-1$^+$ TAMs induced CD8$^+$ T-cell apoptosis and suppressed cytotoxic functions in terms of reducing granzyme B and perforin release. CD8$^+$ T-cell dysfunction has been identified as a mechanism of immune evasion in a broad range of tumors, and the essential extrinsic mechanism of

CD8$^+$ T-cell suppression is the recruitment of TILs that produce multiple inhibitory cytokines and ligands, for instance, TAMs, myeloid-derived suppressor cell, DC, and Tregs.[44] The up-regulation of PD-L1, the canonical checkpoint inhibiting CD8$^+$ T-cell function, in tumor microenvironment is a typical feature of "inflamed cancer" and is an active response to PD-L1 blockade.[45] However, although PD-L1 was highly expressed in TREM-1$^+$ TAMs, we found that anti-PD-L1 treatment failed to inhibit tumor growth and reverse dysfunction and apoptosis in CD8$^+$ T cells with an abundance of TREM-1$^+$ TAMs. In contrast, PD-L1 blockade treatment exhibited significant antitumor efficacy in a mouse tumor model with fewer TREM-1$^+$ TAMs. These results suggested that TREM-1$^+$ TAMs endow anti-PD-L1 resistance, which is frequently found in various cancers, and accounts for the fact that most patients do not benefit from PD-L1/PD-1 blockade.[41] In this process, CD8$^+$ T-cell functions were probably suppressed through a pathway separate from PD-L1/PD-1 axis in the TREM-1$^+$ TAMs context.

Dysfunctional or exhausted CD8$^+$ T cells, which coexpress PD-1 and LAG-3, are regarded as incapable of proliferating and performing cytotoxic functions, characterized by reduced release of granzyme B, perforin, interferon-γ, and so on.[46] However, blocking PD-1/PD-L1 axis alone is not sufficient to protect CD8$^+$ T cells from exhaustion.[47] In line with that conclusion, we found that PD-1$^+$LAG-3$^+$CD8$^+$ T cells and the apoptosis of CD8$^+$ T cells could not be attenuated by PD-L1 blockade in the presence of abundant TREM-1$^+$ TAMs, whereas the opposite result was observed in the Control M group. Thus, we
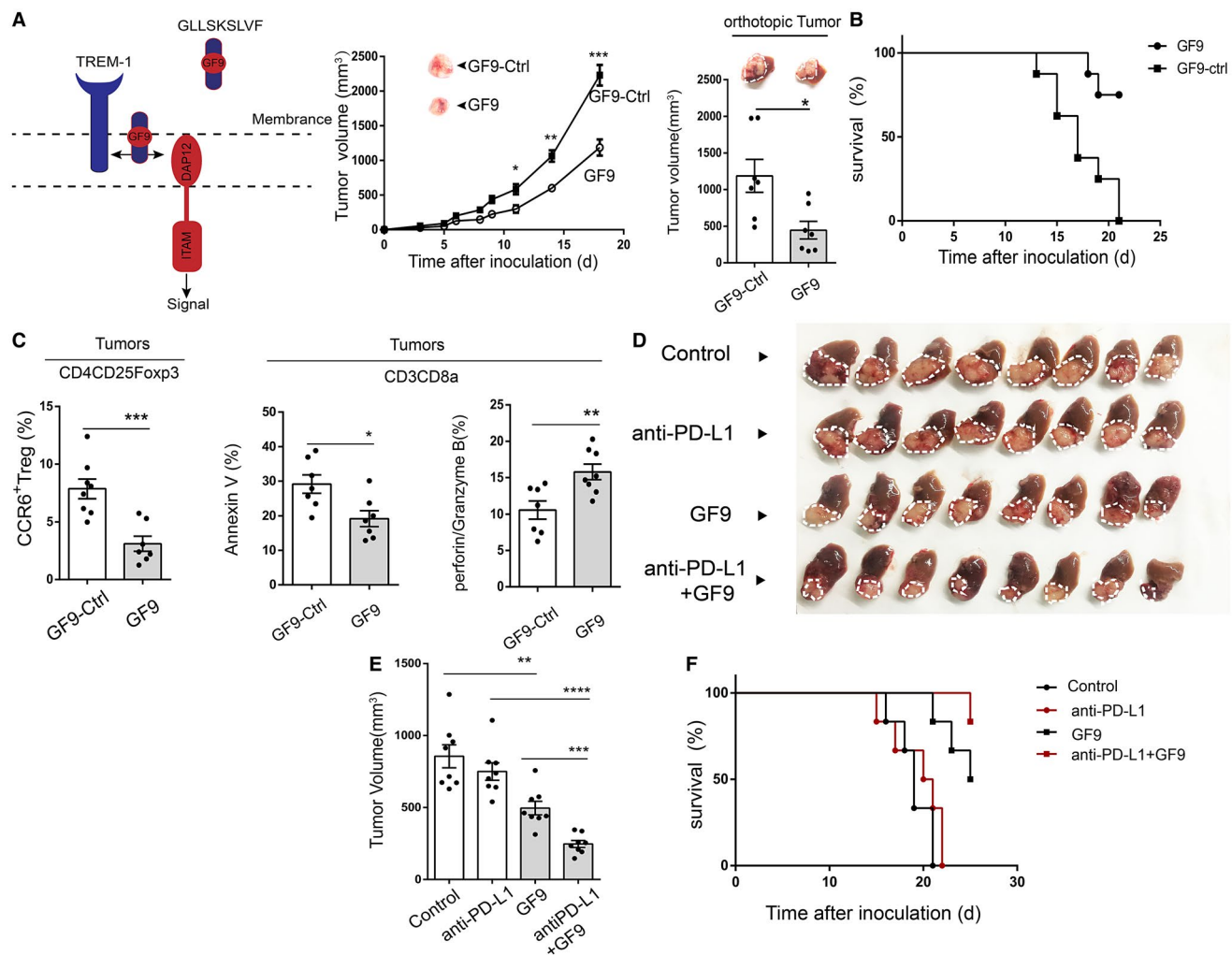
FIG. 6. Blocking TREM-1^{+} TAMs by GF9 attenuates tumor growth and promotes antitumor efficacy of anti-PD-L1 therapy. (A) The schematic of TREM-1 inhibitor GF9 blocking TREM-1 mediated signal (left panel), growth curve of tumor generated by subcutaneous inoculation of hepa1-6 cells after treatment of GF9 (25 mg/kg intraperitoneally) daily (middle panel, n = 6 for each group), and volume of tumor originated from orthotopic inoculation of hepa1-6 cells after treatment of GF9 (25 mg/kg intraperitoneally) daily (right panel, n = 8 for each group). Data are presented as mean ± SD. (B) Overall survival analysis for mice with tumor originated from orthotopic inoculation of hepa1-6 cells after treatment of GF9 (25 mg/kg intraperitoneally) daily (n = 8 for each group). (C) CD4^{+} T and CD8^{+} T cells were isolated from tumor originated from orthotopic inoculation of hepa1-6 cells after treatment of GF9 (25 mg/kg intraperitoneally) daily, and then percentage of CCR6^{+} population of CD4^{+}CD25^{+}Foxp3^{+} Tregs and annexin V^{+} population and granzyme B^{+}/perforin^{+} papulation of CD3^{+}CD8^{+} T cells were analyzed by flow cytometry (n = 7 or 8). Data are presented as mean ± SEM. (D-F) Hepa1-6 cells were inoculated into liver and subjected to treatment of anti-PD-L1 antibody (20 mg/kg intraperitoneally on day 3, 6, and 9) and/ or GF9 (25 mg/kg intraperitoneally) daily. Tumor appearances (D), tumor volume (E, n = 8 for each group), and survival rate of mice (F, n = 6 for each group). Peptide GLLSGSLVF was used as control for GF9 treatment. Data are shown as mean ± SD. *$P < 0.05$; **$P < 0.01$; ***$P < 0.001$; ****$P < 0.0001$.

concluded that the unresponsiveness to PD-L1 blockade was derived from TREM-1^{+} TAM-mediated CD8^{+} T-cell exhaustion. Notably, much importance has been attached to CD4^{+}CD25^{+}Foxp3^{+} Tregs, a substantial suppressive population that impedes effective immune responses by inducing CD8^{+} T-cells

dysfunction and exhaustion.[48] Our immunofluorescent staining and Treg depletion functional assay demonstrated that Foxp3^{+} Treg recruitment that relied on TREM-1^{+} TAMs was an essential process to induce CD8^{+} T-cell exhaustion and PD-L1 blockade resistance. CCL20, the ligand targeting CCR6, was
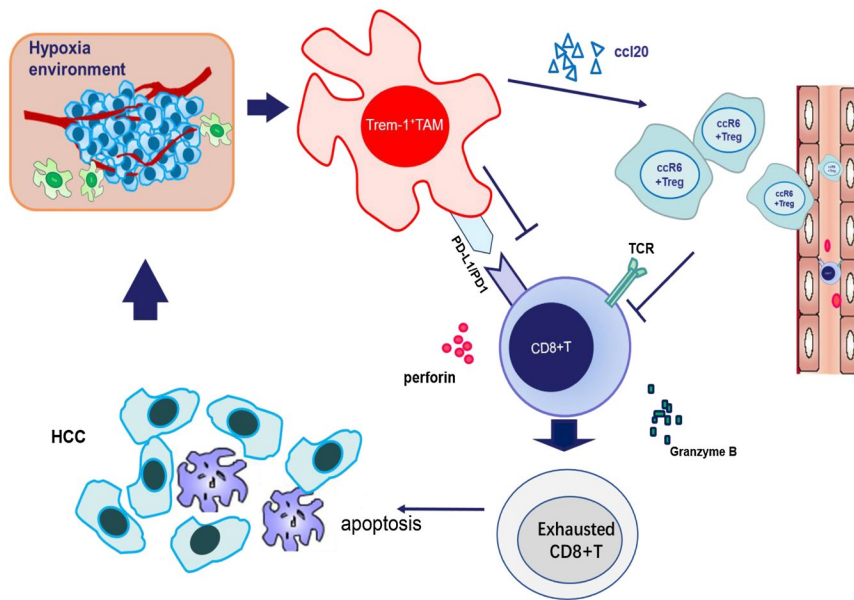
FIG. 7. Schematics depicting that tumor hypoxic environment educates tumor-associated macrophages mediating immunosuppression and PD-L1 resistance.

significantly up-regulated in TREM-1⁺ TAMs and attracted CD4⁺CD25⁺Foxp3⁺ Tregs, which could be strikingly blocked by anti-CCL20 treatment. ERK/NF-κβ pathway activation was mainly responsible for CCL20 expression in TREM-1⁺ TAMs within hypoxic tumor environment. Thus, p65 nuclear translocation seemed to be the most distinct molecular event in this process. Collectively, TREM-1⁺ TAMs recruited CCR6⁺ Tregs, which induced CD8⁺ T-cell exhaustion, through CCL20, dependent on ERK/NF-κβ pathway activation in hypoxic tumor environment, and this process was complementary to the mechanism of anti-PD-L1 resistance and immune escape (Fig. 7). Furthermore, TREM-1 has been determined to be an efficient antitumor target in lung cancer and pancreatic cancer studies.[39,40] In accordance, TREM-1 signal inhibition in TAMs by GF9 treatment strikingly impaired immunosuppression as shown by CCR6⁺ Treg numbers decreasing, a reduction in the apoptosis rate and cytotoxic function improvement in CD8⁺ T cells.

In conclusion, TREM-1⁺ TAM-mediated immunosuppression may be a major biological event for TAMs in hypoxic HCC environment and served as a potential mechanism for anti-PD-L1 therapy resistance. To address the phenomenon that PD-L1 blockade resistance occurred in the presence of TREM-1⁺ TAMs, CCR6⁺ Tregs were revealed to be a key contributor to CD8⁺ T-cell exhaustion and anti-PD-L1 unresponsiveness. The current work demonstrated that TREM-1⁺ TAMs had a high level of PD-L1 and CCL20. Therefore, our results raised the possibility that inhibiting Treg chemotaxis might become an effective approach to attenuate PD-L1 blockade resistance. However, conventional T cells have the ability to transform into Tregs *in situ*, especially in a hypoxic environment.[49] Thus, apart from Tregs trafficking into tumors, other mechanisms that Tregs are present within tumors are urgent to explore to manage Tregs reasonably. Because TREM-1⁺ TAMs were significantly associated with poor prognosis and PD-L1 blockade resistance, blocking TREM-1⁺ TAMs with GF9 provided a promising therapeutic strategy to overcome the resistance to anti-PD-L1 therapy in HCC.

REFERENCES

1) Vaupel P, Mayer A. Hypoxia in cancer: significance and impact on clinical outcome. Cancer Metastasis Rev 2007;26:225-239.

2) **Liang Y**, **Zheng T**, **Song R**, **Wang J**, Yin D, Wang L, et al. Hypoxia-mediated sorafenib resistance can be overcome by EF24 through Von Hippel-Lindau tumor suppressor-dependent HIF-1alpha inhibition in hepatocellular carcinoma. HEPATOLOGY 2013;57:1847-1857.

3) Gilkes DM, Semenza GL, Wirtz D. Hypoxia and the extracellular matrix: drivers of tumour metastasis. Nat Rev Cancer 2014;14:430-439.

4) **Li J**, **Xu Y**, **Long XD**, **Wang W**, Jiao HK, Mei Z, et al. Cbx4 governs HIF-1alpha to potentiate angiogenesis of hepatocellular carcinoma by its SUMO E3 ligase activity. Cancer Cell 2014;25:118-131.

5) Laitala A, Erler JT. Hypoxic signalling in tumour stroma. Front Oncol 2018;8:189.

6) LaGory EL, Giaccia AJ. The ever-expanding role of HIF in tumour and stromal biology. Nat Cell Biol 2016;18:356-365.

7) Noy R, Pollard JW. Tumor-associated macrophages: from mechanisms to therapy. Immunity 2014;41:49-61.

8) **Zhang J**, **Zhang Q**, Lou Y, Fu Q, Chen Q, Wei T, et al. Hypoxia-inducible factor-1alpha/interleukin-1beta signaling enhances hepatoma epithelial-mesenchymal transition through macrophages in a hypoxic-inflammatory microenvironment. HEPATOLOGY 2018;67:1872-1889.

9) Colegio OR, Chu NQ, Szabo AL, Chu T, Rhebergen AM, Jairam V, et al. Functional polarization of tumour-associated macrophages by tumour-derived lactic acid. Nature 2014;513:559-563.

10) Klesney-Tait J, Turnbull IR, Colonna M. The TREM receptor family and signal integration. Nat Immunol 2006;7:1266-1273.

11) Arts RJ, Joosten LA, van der Meer JW, Netea MG. TREM-1: intracellular signaling pathways and interaction with pattern recognition receptors. J Leukoc Biol 2013;93:209-215.

12) **Bosco MC**, **Pierobon D**, Blengio F, Raggi F, Vanni C, Gattorno M, et al. Hypoxia modulates the gene expression profile of immunoregulatory receptors in human mature dendritic cells: identification of TREM-1 as a novel hypoxic marker in vitro and in vivo. Blood 2011;117:2625-2639.

13) Raggi F, Pelassa S, Pierobon D, Penco F, Gattorno M, Novelli F, et al. Regulation of human macrophage M1–M2 polarization balance by hypoxia and the triggering receptor expressed on myeloid cells-1. Front Immunol 2017;8:1097.

14) **Pierobon D**, **Bosco MC**, Blengio F, Raggi F, Eva A, Filippi M, et al. Chronic hypoxia reprograms human immature dendritic cells by inducing a proinflammatory phenotype and TREM-1 expression. Eur J Immunol 2013;43:949-966.

15) Ho CC, Liao WY, Wang CY, Lu YH, Huang HY, Chen HY, et al. TREM-1 expression in tumor-associated macrophages and clinical outcome in lung cancer. Am J Respir Crit Care Med 2008;177:763-770.

16) **Saurer L**, **Zysset D**, Rihs S, Mager L, Gusberti M, Simillion C, et al. TREM-1 promotes intestinal tumorigenesis. Sci Rep 2017;7:14870.

17) Wu J, Li J, Salcedo R, Mivechi NF, Trinchieri G, Horuzsko A. The proinflammatory myeloid cell receptor TREM-1 controls Kupffer cell activation and development of hepatocellular carcinoma. Cancer Res 2012;72:3977-3986.

18) Su S, Liao J, Liu J, Huang D, He C, Chen F, et al. Blocking the recruitment of naive CD4(+) T cells reverses immunosuppression in breast cancer. Cell Res 2017;27:461-482.

19) Nguyen AH, Berim IG, Agrawal DK. Chronic inflammation and cancer: emerging roles of triggering receptors expressed on myeloid cells. Expert Rev Clin Immunol 2015;11:849-857.

20) **Gabrielson A**, **Wu Y**, Wang H, Jiang J, Kallakury B, Gatalica Z, et al. Intratumoral CD3 and CD8 T-cell densities associated with relapse-free survival in HCC. Cancer Immunol Res 2016;4:419-430.

21) Webb JR, Milne K, Watson P, Deleeuw RJ, Nelson BH. Tumor-infiltrating lymphocytes expressing the tissue resident memory marker CD103 are associated with increased survival in high-grade serous ovarian cancer. Clin Cancer Res 2014;20:434-444.

22) Li T, Fan J, Wang B, Traugh N, Chen Q, Liu JS, et al. TIMER: A web server for comprehensive analysis of tumor-infiltrating immune cells. Cancer Res 2017;77:e108-e110.

23) Mantovani A, Marchesi F, Malesci A, Laghi L, Allavena P. Tumour-associated macrophages as treatment targets in oncology. Nat Rev Clin Oncol 2017;14:399-416.

24) Keith B, Johnson RS, Simon MC. HIF1α and HIF2α: sibling rivalry in hypoxic tumour growth and progression. Nat Rev Cancer 2011;12:9-22.

25) Schodel J, Oikonomopoulos S, Ragoussis J, Pugh CW, Ratcliffe PJ, Mole DR. High-resolution genome-wide mapping of HIF-binding sites by ChIP-seq. Blood 2011;117:e207-e217.

26) Cubillos-Zapata C, Avendano-Ortiz J, Hernandez-Jimenez E, Toledano V, Casas-Martin J, Varela-Serrano A, et al. Hypoxia-induced PD-L1/PD-1 crosstalk impairs T-cell function in sleep apnoea. Eur Respir J 2017;50.

27) Noman MZ, Desantis G, Janji B, Hasmim M, Karray S, Dessen P, et al. PD-L1 is a novel direct target of HIF-1alpha, and its blockade under hypoxia enhanced MDSC-mediated T cell activation. J Exp Med 2014;211:781-790.

28) Kuang DM, Zhao Q, Peng C, Xu J, Zhang JP, Wu C, et al. Activated monocytes in peritumoral stroma of hepatocellular carcinoma foster immune privilege and disease progression through PD-L1. J Exp Med 2009;206:1327-1337.

29) Blackburn SD, Shin H, Haining WN, Zou T, Workman CJ, Polley A, et al. Coregulation of CD8+ T cell exhaustion by multiple inhibitory receptors during chronic viral infection. Nat Immunol 2009;10:29-37.

30) Grosso JF, Kelleher CC, Harris TJ, Maris CH, Hipkiss EL, De Marzo A, et al. LAG-3 regulates CD8+ T cell accumulation and effector function in murine self- and tumor-tolerance systems. J Clin Invest 2007;117:3383-3392.

31) Tumeh PC, Harview CL, Yearley JH, Shintaku IP, Taylor EJ, Robert L, et al. PD-1 blockade induces responses by inhibiting adaptive immune resistance. Nature 2014;515:568-571.

32) Maj T, Wang W, Crespo J, Zhang H, Wang W, Wei S, et al. Oxidative stress controls regulatory T cell apoptosis and suppressor activity and PD-L1-blockade resistance in tumor. Nat Immunol 2017;18:1332-1341.

33) **Maruyama T**, **Li J**, Vaque JP, Konkel JE, Wang W, Zhang B, et al. Control of the differentiation of regulatory T cells and T(H)17 cells by the DNA-binding inhibitor Id3. Nat Immunol 2011;12:86-95.

34) Tanaka A, Sakaguchi S. Regulatory T cells in cancer immunotherapy. Cell Res 2017;27:109-118.

35) Colonna M. TREMs in the immune system and beyond. Nat Rev Immunol 2003;3:445-453.

36) Baba M, Imai T, Nishimura M, Kakizaki M, Takagi S, Hieshima K, et al. Identification of CCR6, the specific receptor for a novel lymphocyte-directed CC chemokine LARC. J Biol Chem 1997;272:14893-14898.

37) Anand RJ, Gribar SC, Li J, Kohler JW, Branca MF, Dubowski T, et al. Hypoxia causes an increase in phagocytosis by macrophages in a HIF-1alpha-dependent manner. J Leukoc Biol 2007;82:1257-1265.

38) Liu FQ, Liu Y, Lui VC, Lamb JR, Tam PK, Chen Y. Hypoxia modulates lipopolysaccharide induced TNF-alpha expression in murine macrophages. Exp Cell Res 2008;314:1327-1336.

39) Shen ZT, Sigalov AB. Novel TREM-1 inhibitors attenuate tumor growth and prolong survival in experimental pancreatic cancer. Mol Pharm 2017;14:4572-4582.

40) Sigalov AB. A novel ligand-independent peptide inhibitor of TREM-1 suppresses tumor growth in human lung cancer xenografts and prolongs survival of mice with lipopolysaccharide-induced septic shock. Int Immunopharmacol 2014;21:208-219.

41) Kim JM, Chen DS. Immune escape to PD-L1/PD-1 blockade: seven steps to success (or failure). Ann Oncol 2016;27: 1492-1504.

42) Rohwer N, Cramer T. Hypoxia-mediated drug resistance: novel insights on the functional interaction of HIFs and cell death pathways. Drug Resist Updat 2011;14:191-201.

43) Li KK, Adams DH. Antitumor CD8+ T cells in hepatocellular carcinoma: present but exhausted. Hepatology 2014;59: 1232-1234.

44) Jiang Y, Li Y, Zhu B. T-cell exhaustion in the tumor microenvironment. Cell Death Dis 2015;6:e1792.

45) **Zou W**, **Wolchok JD**, **Chen L**. PD-L1 (B7–H1) and PD-1 pathway blockade for cancer therapy: Mechanisms, response biomarkers, and combinations. Sci Transl Med 2016;8: 328rv4.

46) Anderson AC, Joller N, Kuchroo VK. Lag-3, Tim-3, and TIGIT: Co-inhibitory receptors with specialized functions in immune regulation. Immunity 2016;44:989-1004.

47) **Woo SR**, **Turnis ME**, **Goldberg MV**, Bankoti J, Selby M, Nirschl CJ, et al. Immune inhibitory molecules LAG-3 and PD-1 synergistically regulate T-cell function to promote tumoral immune escape. Cancer Res 2012;72:917-927.

48) Shevach EM. Mechanisms of foxp3+T regulatory cell-mediated suppression. Immunity 2009;30:636-645.

49) **Clambey ET**, **McNamee EN**, Westrich JA, Glover LE, Campbell EL, Jedlicka P, et al. Hypoxia-inducible factor-1 alpha–dependent induction of FoxP3 drives regulatory T-cell abundance and function during inflammatory hypoxia of the mucosa. Proc Natl Acad Sci U S A 2012;109:E2784-E2793.

Author names in bold designate shared co-first authorship.

Supporting Information

Additional Supporting Information may be found at onlinelibrary.wiley.com/doi/10.1002/hep.30593/suppinfo.